Influence of Solid Friction on Polymer Relaxation in Gel Electrophoresis

Sergei Burlatsky; John Deutch

Science, New Series, Vol. 260, No. 5115 (Jun. 18, 1993), 1782-1784.

Influence of Solid Friction on Polymer Relaxation in Gel Electrophoresis

Sergei Burlatsky and John Deutch

Solid friction between a charged polymer and fixed gel points can dramatically affect polymer mobility in gel electrophoresis. The effect is present when a polymer chain is entangled over many gel points along a portion of its length, leading to significantly different behavior than predicted by conventional theory: the mobility of the chain decreases and exhibits a stronger length dependence, which separates long linear charged polymers of different molecular weights.

There is considerable interest in understanding (*1*) the mechanism of DNA electrophoresis because of its importance to molecular biology [for recent reviews see (*2–4*)]. In electrophoresis, the success of the separation of the charged polymer chains of different lengths is directly related to the time required for the external electric field E to drag the chain through the fixed obstacles that characterize the gel. In previous theoretical work (*5–17*) and computer simulations (*18–25*), the mechanism responsible for the movement has been attributed to viscous friction between the chain and the solvent as the chain moves along a random path defined by its conformation among the fixed obstacles of the gel network. The gel itself is not treated as a friction source.

At the molecular level, the electric field forces polymer segments against the gel fibers, which dissipates energy by distortion of the gel fibers, displacement of solvent, and transfer of mechanical energy between local vibrations. These effects are manifest as friction in addition to the friction that exists between the polymer and the solvent. We examined the consequences of friction between the moving segments of the polymer chain and the fixed gel based on a simple model of solid friction. For important configurations of the polymer chain, the solid friction dramatically changes the dynamics of the polymer chain. Experimental results for the mobility of polymer chains as a function of length in pulsed electrophoresis cannot be understood without consideration of solid-like friction.

Solid friction arises when an object moves across a surface (Fig. 1A). On a macroscopic scale, the frictional force $\mathbf{F}_{\mathrm{rub}}$ is directed opposite the direction of the chain motion $\mathbf{v}$ and is equal in magnitude to the normal force $\mathbf{N}$ exerted by the object on the surface times a dimensionless coefficient of sliding friction μ; this solid friction force is independent of contact area (*26*). For a polymer chain entangled in a gel, this normal force is proportional to the tension on the chain and thus greatly modifies the chain dynamics.

In the conventional picture of electrophoresis, an extended polymer chain, which is assumed to be uniformly charged, is dragged free from entanglement about a fixed gel point by the action of the external electric field $\mathbf{E}$ (Fig. 1B). In the absence of solid friction, this picture is similar to a rope being pulled over a frictionless peg through a viscous medium; the velocity with which the rope is withdrawn is determined by a balance of the viscous drag and the tension imposed by the external field. In the presence of solid friction, this velocity is reduced by the rubbing force exerted at the point of contact between the moving rope and the fixed peg.

An interesting configuration is that which is "U" shaped (*12, 16*) (Fig. 2), which is believed to be important in pulsed electrophoresis (*12, 15, 16*). The contribution of solid friction is sensitive to the configuration, but the viscous drag, in the absence of hydrodynamic interaction, is not. In this configuration, the arms of length L_1 and L_3 are leaking from an entangled region of length L_2, oriented for simplicity perpendicular to the external electric field. This physical situation is envisioned in most off-lattice computer simulation studies (*10, 15, 18–22*), and similar configurations have been observed experimentally (*27, 28*).

As the polymer chain is dragged through the gel points, the tension along the chain $T(r)$ must overcome the solid friction that arises from the chain segments rubbing over the fixed gel points. Not every segment will be in contact with a gel point if the polymer segment size b is smaller than the characteristic separation between gel points a. In the entangled region, the polymer chain is extended among many obstacles of the gel (Fig. 3). The chain makes different angles at the interaction points, $0 < \vartheta_n < \pi$, and the local $\cos(\vartheta_n/2)$ is always positive.

Over a coarse-grained distance along the chain, the average solid friction rubbing force changes the tension along the chain. The magnitude of the average rubbing friction force F_{rub} can be approximated as $\mu\varepsilon T[r(n)]2\langle\cos(\vartheta_n/2)\rangle$, where ε is a factor that takes into account the likelihood that segment n interacts with a gel point and the angular bracket indicates an average of the possible angles of the chain rubbing against a particular gel point. Strictly, the value of the average cosine depends on the history of the chain in the electric field. In a pulsed electrophoretic experiment, the chain has a random orientation at the beginning of the pulse, and $\langle\cos(\vartheta_n/2)\rangle$ is approximately $2/\pi$. After a long time in a large static field, the chain approaches complete elongation and $\langle\cos(\vartheta_n/2)\rangle$ approaches zero. One could design a pulse sequence that would make this average large.

We consider a polymer chain that is stretched in a randomly configured tube within the gel, which is appropriate for the pulsed or small constant field experiments, and introduce a constant factor $\alpha = \varepsilon\langle\cos(\vartheta_n/2)\rangle$. Accordingly, the magnitude of the solid friction force arising from the chain passing through this coarse-grained distance is

$$F_{\mathrm{rub}}[r(n,t)] = \mu\alpha T[r(n)] \qquad (1)$$

The steady flow of the charged polymer through the gel is determined by balancing the forces over a small interval ($2\delta r$ in Fig. 3) along the entangled chain. The change in tension along the chain balances the external force, the frictional force from the solvent, and the rubbing friction. With the sign conventions as presented in Fig. 3, the pertinent equation is

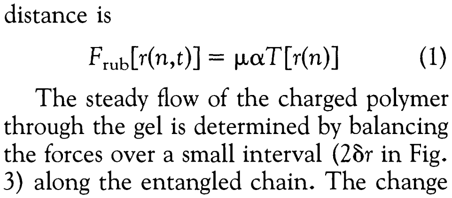

Fig. 1. (**A**) Mechanical concept of sliding solid friction. The solid object is pulled across a flat surface with velocity **v**. There is an opposing friction force, independent of the velocity and surface area that equals μ**N**. The reaction force **N** is equal and opposite to all forces that act on the object perpendicular to the plane. In our case, for an entangled polymer chain, the magnitude of this force *N* will be proportional to the local tension *T*(*r*). (**B**) An extended polymer chain configured about a single, fixed gel point. The chain is pulled by the force an external electric field exerts on the charge distributed along the polymer segments. The local tension *T*(*r*) that presses the polymer chain against the gel point is indicated.

Department of Chemistry, Massachusetts Institute of Technology, Cambridge, MA 02139.

$$\frac{dT(r)}{dr} = \rho Eq\cos\theta - \rho\beta v - \alpha\rho\mu T(r) \quad (2)$$

where β is the friction coefficient of each segment, q is the charge per segment, ρ is the segment density along the stretched chain (assumed constant), and θ is the angle between the external field and the tangent to the polymer chain at point r. This is the central equation of our analysis; it includes the effect of the solid friction in the term that is proportional to the sliding friction coefficient μ. The equation is only valid for positive v because the solid friction force acts opposite the direction of motion. The effect of intersegment forces can also be included (*29*). In the absence of solid friction, Eq. 2 is the commonly accepted equation of motion with thermal fluctuation omitted (*10, 12*). A detailed derivation of a general expression for the steady state of an entangled chain in an arbitrary configuration (*30*) is possible.

For the U-shaped configuration (*12, 16*) (Fig. 2), the effect of solid friction is only present in the central arm, which is perpendicular to the electric field. The steady-state flux v is found by solving Eq. 2 subject to the boundary conditions $T(0) = \rho(Eq - \beta v)L_1$ and $T(L_2) = -\rho(Eq + \beta v)L_3$. The result is only valid for v greater than or equal to zero.

$$\beta v = qE[L_1 \exp(-\alpha\rho\mu L_2) - L_3]/ \left[L_1 \exp(-\alpha\rho\mu L_2) + L_3 + L_2 \frac{1 - \exp(-\alpha\rho\mu L_2)}{\alpha\rho\mu L_2}\right] \quad (3)$$

Several cases follow from Eq. 3:

1) If $L_1 > L_3 \exp[\alpha\mu\rho L_2]$, the chain moves with a velocity that extends the larger arm L_1 until the entire chain leaks from the entangled region. However, if $L_3 < L_1 < L_3 \exp[\alpha\mu\rho L_2]$, then the solution to Eq. 2 is $v = 0$, which indicates that the chain is frozen (*31*). There is no value of the external electric field that can overcome the solid friction from the entangled region given the lengths of the entangled region (L_2) and the advancing (L_1) and receding (L_3) arms. Solid friction predicts freezing of chain configurations; this freezing does not arise in the conventional picture.

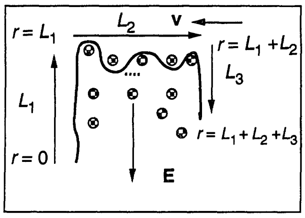

Fig. 2. Polymer chain in U-shaped configuration with unequal arms caught over several gel points. The external electric field **E** is directed downward. The distance from the end of the chain, r, is indicated at four points.

2) In the limit of no solid friction ($\mu \rightarrow 0$), Eq. 3 leads to the expected result (*15, 16, 18*)

$$\beta v = Eq \frac{(L_1 - L_3)}{(L_1 + L_2 + L_3)} \quad (4)$$

which shows that the flux is proportional to the difference in length of the dangling chain ends along the field direction. If $L_2 \rightarrow 0$, the expression for v in Eq. 3 reduces to the form of Eq. 4 without solid friction and $L_2 = 0$, as expected from simulation results of chains trapped about a single gel point (*15, 16, 18*). Solid friction slows down chain leakage only when there is entanglement over a finite distance (*32*). In previous work it was assumed that slow mobility arises from a small net electric force that is attributable to nearly identical initial lengths of the arms of the chain wrapped about a single gel obstacle. However, Smith and Bendich (*27*) observed directly that such configurations soon slip off. In contrast, open circular DNA migrates much more slowly (*33*), which we attribute to entanglement and resulting solid friction.

3) The experimental significance of solid friction is clearly illustrated by the results of leakage from U configurations. Successful separation requires length dependence of the mobility μ_{mob}, so that solid friction discriminates chains of different lengths. The mobility is $\bar{v}/E$, where $\bar{v}$ is the average velocity over the length L_1 as the chain leaks from the entangled region. This average velocity is

$$\bar{v} = \frac{1}{L - L_{\text{min}}} \int_{L_{\text{min}}}^{L} dL_1 v(L_1) \quad (5)$$

where L_{min} is the minimum length for which leakage along L_1 begins, and L is the total polymer chain length.

Consider the limiting case where $L_3 = 0$ and $L_{\text{min}} = 0$. If there is no solid friction, then $\mu_{\text{mob}} = \bar{v}/E = q/2\beta$ according to Eq. 5, which is of the same order as the value for a free-draining solution and is independent of chain length. On the other hand, if solid friction is present, then according to Eq. 4, there is significant reduction in this average velocity and mobility, and they are both length-dependent (Fig. 4). Available experimental information (*34*) at low static fields but high gel concentration, where strong entanglement is expected, indicates a decline of mobility with long chain length greater than that predicted by biased reptation theory (*6–9, 13*).

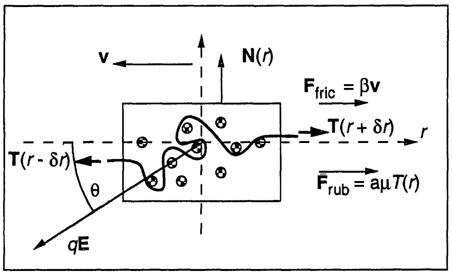

Fig. 3. The direction of various forces acting on a coarse-grained element of the polymer chain. The steady-state segment velocity is in the $(-r)$ direction, so the frictional forces $\mathbf{F}_{\text{rub}}$ and $\mathbf{F}_{\text{fric}}$ are in the $(+r)$ direction. The distance δr is along the coarse-grained polymer chain.

The existing model of gel electrophoresis is based on several simple qualitative ideas that are evident simplifications in that the stiffness of the charged particle chains, the hydrodynamic interaction between the gel and polymer segments, and the finite size of the polymer segments are ignored. Our purpose here is to point out a qualitative effect that, even when treated simply, leads to very different behavior than is predicted by the standard picture. Insight will undoubtedly come from computer simulations that include explicitly some inelastic interaction between the moving polymer chain and the background gel network (*35*).

We expect the effect of solid friction on mobility to be most pronounced in pulsed alternating electric field electrophoresis, in a regime where the chain length is large compared to the average distance between gel points. This prediction should be confirmed by future experimental or simulation studies. Further, we speculate that solid friction is less important in polymer melts in which individual chains can move more freely than in a fixed gel network. In reality, solid friction could be mitigated by deformation of the gel fibers by the polymer chain or lubrication by the solvent (*36*). However, if present, the influence of solid friction should lead to quite different ef-

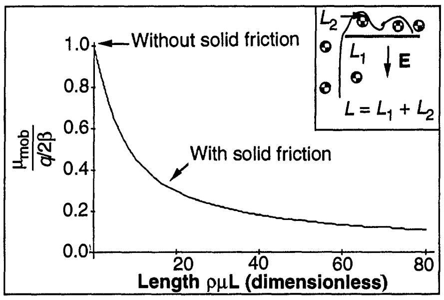

Fig. 4. Dimensionless mobility and average flux ($\mu_{\text{mob}} = v/E$) for leakage from U-shaped polymer configuration in the gel. The leakage begins with the entire polymer of length L entangled in the direction perpendicular to the field and ends with the entire polymer aligned parallel to the field. The physical situation is depicted in Fig. 2 and the equation for $v(L_1)$ is given in Eq. 3 with L_3 equal to zero.

fects, such as elastic waves in the gel (microsound) and local heating.

REFERENCES AND NOTES

1. See J. Maddox [*Nature* **345**, 381 (1990)] and A. Khurana [*Phys. Today* **240** (no. 8), 20 (1990)] for popular accounts of theoretical developments.
2. B. Norden, C. Elvingson, M. Jonsson, B. Akerman, *Q. Rev. Biophys.* **24**, 103 (1991).
3. J. L. Viovy, T. Dyke, F. Caron, *Contemp. Phys.* **33**, 25 (1992).
4. B. H. Zimm and S. D. Levene, *Q. Rev. Biophys.* **25**, 171 (1992).
5. L. S. Lerman and H. L. Frisch, *Biopolymers* **21**, 995 (1982).
6. O. J. Lumpkin and B. H. Zimm, *ibid.*, p. 2315.
7. O. J. Lumpkin, P. Dejardin, B. H. Zimm, *ibid.* **24**, 1573 (1985).
8. G. W. Slater and J. Noolandi, *Phys. Rev. Lett.* **55**, 1579 (1985); *Biopolymers* **25**, 431 (1986).
9. J. Noolandi, J. Rousseau, G. W. Slater, *Phys. Rev. Lett.* **58**, 2428 (1987).
10. J. M. Deutsch, *ibid.* **59**, 1255 (1987); *Science* **240**, 922 (1988).
11. J. L. Viovy, *Phys. Rev. Lett.* **60**, 855 (1988).
12. J. Noolandi, G. W. Slater, H. A. Lim, J. L. Viovy, *Science* **243**, 1456 (1989).
13. P. Dejardin, *Phys. Rev. A* **40**, 4752 (1989).
14. B. H. Zimm, *Phys. Rev. Lett.* **61**, 2965 (1988); *J. Chem. Phys.* **94**, 2187 (1991).
15. J. M. Deutsch, *J. Chem. Phys.* **90**, 7436 (1989).
16. H. A. Lim, G. W. Slater, J. Noolandi, *ibid.* **92**, 709 (1990).
17. J. M. Schurr and S. B. Smith, *Biopolymers* **29**, 1161 (1990).
18. M. O. de la Cruz, J. M. Deutsch, S. F. Edwards, *Phys. Rev. A* **33**, 2047 (1986); these authors explicitly assume frictionless contact between the polymer and the gel.
19. M. O. de la Cruz, D. Gersappe, E. O. Shaffer, *Phys. Rev. Lett.* **64**, 2324 (1990).
20. E. O. Shaffer and M. O. de la Cruz, *Macromolecules* **22**, 1351 (1989).
21. T. A. J. Duke, *Phys. Rev. Lett.* **62**, 2877 (1989); *J. Chem. Phys.* **93**, 9055 (1990).
22. T. L. Madden and J. M. Deutsch, *J. Chem. Phys.* **94**, 1584 (1991).
23. J. M. Deutsch and J. D. Reger, *ibid.* **95**, 2065 (1991).
24. T. A. J. Duke and J. L. Viovy, *Phys. Rev. Lett.* **68**, 542 (1992); *J. Chem. Phys.* **96**, 8552 (1992).
25. G. W. Slater, *J. Phys. II* **2**, 1149 (1992).
26. N. H. Frank, *Introduction to Mechanics and Heat* (McGraw-Hill, New York, 1939), p. 55.
27. S. B. Smith and A. J. Bendich, *Biopolymers* **29**, 1167 (1990).
28. S. B. Smith, P. K. Aldridge, J. B. Callis, *Science* **243**, 203 (1989).
29. Intersegment forces can be included. For example, for elastic forces, the tension in Eq. 4 would be replaced by:
$$T(r) = -\gamma \frac{dr(n)}{dn}$$
where γ is the elastic force constant, and $\rho = dn/dr$ and ε are no longer constant.
30. The general result for the steady-state velocity of an entangled chain through a coarse-grained tube of length L with tension $T(0)$ at one end and $T(L)$ at the other end is
$$\frac{\beta v}{\alpha\mu} = \frac{\exp(-\alpha\mu\rho L)T(0) - T(L)}{1 - \exp(-\alpha\mu\rho L)} + \frac{qE\int_0^L \exp(\alpha\mu\rho x)\cos[\theta(x)]dx}{\exp(\alpha\mu\rho L) - 1}$$
Trapping of the entangled chain occurs from regions where $\cos[q(x)]$ is negative.
31. When the segment velocity approaches zero, it is necessary to take into account the influence of thermal fluctuation, which is not included in our analysis. These thermal fluctuations lead to polymer motion, therefore modifying the results quoted here as $v \rightarrow 0$.
32. The coarse graining excludes end effects, which lead to small corrections that do not depend on polymer length.
33. S. D. Levene and B. H. Zimm, *Proc. Natl. Acad. Sci. U.S.A.* **84**, 4054 (1987).
34. C. R. Calladin, C. M. Collis, H. R. Drew, M. R. Mott, *J. Mol. Biol.* **221**, 981 (1991); see also E. Avranitdou and D. Hoagland, *Phys. Rev. Lett.* **67**, 1461 (1991) and D. L. Smisek and D. A. Hoagland, *Science* **248**, 1221 (1990).
35. In some off-lattice simulations (*18–22*), the rules for chain movement include rejection of the move (in contrast to elastic reflection) if the chain encounters a gel point. This approach implicitly corresponds to an inelastic collision, which is required for solid friction.
36. The temperature dependence of the mobility could be quite different if solid friction is present in addition to viscous friction from the solvent.
37. J.D. thanks G. M. Whitesides for helpful discussions.

29 January 1993; accepted 16 April 1993

A Bimetallic Hydroformylation Catalyst: High Regioselectivity and Reactivity Through Homobimetallic Cooperativity

Melanie E. Broussard, Booker Juma, Spencer G. Train,
Wei-Jun Peng, Scott A. Laneman, George G. Stanley*

The *racemic* and *meso* diastereomers of an electron-rich binucleating tetraphosphine ligand have been used to prepare homobimetallic rhodium norbornadiene complexes. The *racemic* bimetallic Rh complex is an excellent hydroformylation catalyst for 1-alkenes, giving both a high rate of reaction and high regioselectivity for linear aldehydes, whereas the *meso* complex is considerably slower and less selective. A mechanism involving bimetallic cooperativity between the two rhodium centers in the form of an intramolecular hydride transfer is proposed. Mono- and bimetallic model complexes in which the possibility for bimetallic cooperativity has been reduced or eliminated are very poor catalysts.

Hydroformylation (also called "oxo"), the world's largest industrial homogeneous catalytic process, produces more than 5 billion kilograms of aldehydes and alcohols each year (*1*). In this process, alkenes react with hydrogen and carbon monoxide to give either linear or branched aldehydes (Eq. 1; R, alkyl).

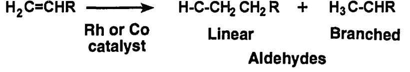

$$H_2C{=}CHR \xrightarrow[\text{Rh or Co catalyst}]{H_2,\ CO} \underbrace{\underset{\text{Linear}}{H\text{-}\overset{\overset{O}{\|}}{C}\text{-}CH_2CH_2R} + \underset{\text{Branched}}{H_3C\text{-}\overset{\overset{O=C-H}{|}}{C}HR}}_{\text{Aldehydes}} \qquad (1)$$

Monometallic rhodium triphenylphosphine (Rh/PPh_3) catalysts dominate the industry, particularly for C_3 through C_6 1-alkenes, where regioselectivity in making the more valuable linear aldehyde products is critical.

Demonstrating that two or more metal centers can cooperate in a homogeneous catalytic process to produce a better catalyst compared to monometallic systems has been a major goal of our research. Several groups have reported dimer and cluster catalysis of hydroformylation (*2*). None of these polymetallic catalysts, however, combine high product regioselectivities with high reaction rates, and none of them compare favorably to commercial Rh/PPh_3 monometallic catalysts. We have designed a tetraphosphine ligand that can simultaneously bridge and chelate two metal centers to create bimetallic complexes with considerable conformational flexibility. This ligand, $(Et_2PCH_2CH_2)(Ph)PCH_2P(Ph)(CH_2CH_2PEt_2)$ (et,ph-P4; Et, ethyl), has *racemic* (**1r**) and *meso* (**1m**) diastereomers (*3*). We have characterized bimetallic complexes of **1r** and **1m** in which the two metals are separated or bonded to one another (*4*).

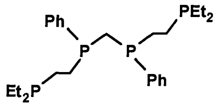

***racemic* - et,ph-P4**
1r

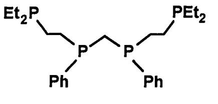

***meso* - et,ph-P4**
1m

The reaction of **1r** or **1m** (*5*) with two equivalents of $[Rh(nbd)_2](BF_4)$ (nbd = norbornadiene) produces the bimetallic complexes $[Rh_2(nbd)_2(et,ph\text{-}P4)](BF_4)_2$ (*racemic* **2r**, and *meso* **2m**) in high yield (*6*). An x-ray crystal structure determination (*7*) of **2r** (Fig. 1) shows that the et,ph-P4 ligand bridges and chelates the two square-planar Rh centers, as observed in previous bimetallic complexes of et,ph-P4. There is no Rh–Rh bonding in this complex, and the metals are separated by 5.505 Å. The ^1H and ^{31}P nuclear magnetic resonance (NMR) spectra for **2m** point to a bridged and chelated bimetallic structure similar to

---

Department of Chemistry, Louisiana State University, Baton Rouge, LA 70803-1804.

*To whom correspondence should be addressed.